Stabilization and characterization of Pt nanoparticles on HOPG

Halvorsen, Helga; Bock, C.; MacDougall, Barry; Tanaka, N.; Wang, D.

ECS Transactions, 11 (31) 75-86 (2008)
10.1149/1.2953509 ©The Electrochemical Society

Stabilization and Characterization of Pt Nanoparticles on HOPG

H. Halvorsen[a,b], C. Bock[b], B. MacDougall[a,b], and D. Wang[b]

[a] Department of Chemistry, University of Ottawa, Ottawa, Ontario K1N 6N5, Canada
[b] Institute for Chemical Process and Environmental Technology, National Research Council, Ottawa, Ontario, K1A 0R6, Canada

Platinum nano-catalysts are deposited, either by electrodeposition at constant potential or thermal decomposition, onto highly ordered pyrolytic graphite (HOPG). To help stabilize the nano-catalyst, the HOPG substrate is oxidized either by electrochemical methods or by ozone gas. The combination of two deposition techniques and two substrate oxidation techniques results in four different types of samples. As a point of reference, the particle morphology, activity towards oxidation of adsorbed carbon monoxide, and electrochemical stability of the four different types of samples are compared to a sample made by electrodeposition of Pt onto freshly cleaved HOPG. Of the four samples prepared, the combination of thermal reduction onto ozone oxidized HOPG was found to produce the most stable platinum nano-catalyst.

Introduction

Platinum is used to catalyze a vast number of heterogeneous reactions including hydrogenation, dehydrogenation, isomerisation, reduction, and oxidation reactions (1). It is platinum's high activity towards oxidizing hydrogen and simple organics such as methanol, as well as reducing oxygen, that renders it an important catalyst for low temperature energy conversion technologies such as polymer electrolyte membrane fuel cells (PEMFCs) and direct methanol fuel cells (DMFCs). Due to the high cost of platinum, methods of increasing the activity of platinum catalysts, and hence, decreasing the system cost, are crucial for the successful implementation of these fuel cell technologies.

Heterogeneous catalytic reactions take place on the surface of a catalyst. Decreasing the particle size results in a higher surface area per unit weight of catalyst material, and hence, an increase in measured activity per unit weight of catalyst material (i.e., mass activity) may be expected. However, a simple relationship between mass activity and platinum particle size is not typically observed. In fact, mass activity often maximizes at a particle size of 3.5 – 4 nm. This particle-size effect is well documented for numerous reactions such as the CH_3OH oxidation and the O_2 reduction reaction (ORR) (2,3,4). Various theories concerning changes in the geometric characteristics of nanometre-sized particles or diffusion effects ruled by inter-particle distances have been put forward to explain the particle-size effect (5,6). However, definitive experimental verification of these theories has not yet been achieved, partly due to the lack of existing model catalyst systems. A model catalyst system, appropriate for a particle-size effect study, is one where the catalyst is synthesized with a narrow particle size distribution, where the size can be varied from 1 to 10 nm, and where the catalyst is free from all possible sources of

interference during catalytic activity testing. The development of an ideal model catalyst system is the motivation for this research.

In this work, electrodeposition and thermal decomposition of Pt onto HOPG is investigated. Oxidation of the HOPG substrate is carried out in order to stabilize the Pt nano-catalyst. Substrate oxidation methods utilized in this work are electrochemical oxidation or oxidation with ozone gas. The combination of two deposition techniques and two substrate oxidation techniques results in four different types of samples that are studied with respect to morphology, activity towards the electrochemical oxidation of adsorbed CO (CO_{ads}), and electrochemical stability.

Experimental

Solutions, Cells, and Electrodes

All solutions were made by volume using high resistivity 18 MΩ water. A three compartment cell with the reference electrode separated from the working- and counter-electrode by a Luggin capillary was employed for the electrochemical deposition of Pt. A Hg/Hg_2SO_4, 0.5 M H_2SO_4 (MSE) electrode was used as the reference electrode. All potentials reported in this paper are reported vs. the MSE. A large surface area Pt mesh was used as the counter electrode. Electrochemical experiments were performed using an EG&G 273 potentiostat driven by CorrWare software program (Scribner, Assoc.).

Nano-catalyst Preparation

Electrochemical deposition of Pt onto HOPG (SPI supplies, grade SPI-1) was carried out in solutions consisting of 1 mM $PtCl_4$ (Alfa Aesar 99.9 % purity) and 0.1 M H_2SO_4 as supporting electrolyte. Pt was electrodeposited at constant potential onto freshly cleaved, ozone oxidized, or electrochemically oxidized HOPG in this work. The HOPG substrate was placed in a sample holder exposing 0.38 cm^2 of geometric surface area for deposition; all electrodeposition currents are normalized to this area. To prevent spontaneous reduction of platinum onto the HOPG substrates, the working electrode was immersed and removed from the platinum salt solution while the potential was held at + 0.25 V (7,8,9). Electrochemical deposition was initiated by stepping the potential from + 0.25 to – 0.475 V and terminated by stepping the potential back to + 0.25 V. The deposition potential was selected as to maximize the overpotential yet to ensure that H_2 evolution was not occurring. Deposition times ranged from 2.5 to 60 s. All solutions were deoxygenated with high purity argon prior to deposition. Once the HOPG was removed from the deposition solution it was immediately rinsed with 18 MΩ water. All samples were kept in a desiccator until further analysis.

Thermal decomposition was achieved by pipetting a solution of H_2PtCl_4 and HCl onto freshly cleaved, ozone oxidized, or electrochemically oxidized HOPG. Once air dried, the sample was placed under a flow of hydrogen gas (8% H_2 in Ar) at 250 °C. XPS analysis (not shown) indicated that reduction conditions were sufficient to reduce the platinum salt to platinum metal.

Oxidation of HOPG

Ozone oxidation of HOPG was carried out according to work by Tracz, et al. (10). A Model 49C ozone analyzer equipped with and optional ozone generator was used to generate 0.15 ppm O_3. Zero air was fed into the ozone analyzer generating an ozone/air mixture, which then flowed to the reaction chamber (a quartz tube of 22 mm inner diameter that was placed in the center of a 300 ºC tube furnace). The ozone/air flow could be switched from flowing to the reaction chamber or to a vent using a three way glass stopcock, thus allowing precise control of the oxidation times. The HOPG substrates were heated at 300 °C in an air atmosphere for 5 min. prior to O_3 oxidation. Following the oxidation period, the oven was switched off and the ozone/air mixture was flushed out of the tube furnace with zero air for an additional 5 min. The samples were allowed to cool to room temperature at the edge of the tube furnace. Teflon tubing was used to transport the ozone/air mixture to the tube furnace. Ozone oxidized HOPG samples were analyzed by scanning tunnelling microscopy (STM) in ambient air at room temperature the same day of preparation using a Pico SPM from Molecular Imaging.

Electrochemical oxidation of HOPG occurred in a solution of 0.1 M H_2SO_4 at 1.55 V vs. MSE. Oxidation times ranged from 30 to 180 s. Electrochemically oxidized HOPG samples were analyzed by scanning electron microscopy using a JEOL 840A scanning electron microscope. All photos were taken using an accelerating voltage of 20 kV and a working distance of 15 mm.

Particle Size/Morphology Determination

The size and morphology of electrochemically deposited platinum were determined by transmission electron microscopy (TEM). TEM samples were prepared by gluing a Cu grid to the surface of the Pt/HOPG samples using a small amount of Vishay Micro-measurements 610 bond. After curing the glue for 1 h at 100 °C, the Cu grids were peeled off the HOPG surface. Small flakes of HOPG remained attached to the grid and TEM analysis was performed on these HOPG flakes. To determine if heating the sample at 100 °C for 1 h affected the platinum nanoparticles, one sample was prepared using Krazy Glue® cured at room temperature. Comparison of the samples prepared using 610 bond and Krazy Glue® indicated that heating the samples to 100 °C for one hour had no effect on platinum morphology. 610 bond allowed for easier sample preparation and therefore was used for all TEM analysis. Due to the destructive nature of the TEM sample preparation, the same sample could not be imaged before and after electrochemical analysis. A Philips CM 20 TEM was employed to measure the size of the Pt catalysts.

Adsorbed Carbon Monoxide (CO_{ads}) Stripping Voltammetry

Carbon monoxide was adsorbed onto Pt catalysts at – 0.54 V by bubbling CO gas (Matheson purity, Matheson gas) through a 0.5 M H_2SO_4 solution for 10 min. The solution was then purged of CO by bubbling argon gas for 30 min, while maintaining the potential at – 0.54 V. To remove the CO_{ads} the potential was cycled from – 0.54 to 0.4 V at 10 mV s^{-1}. The positive potential scan was limited to 0.4 V to prevent the Pt catalyzed surface oxidation of HOPG (11,12,13). Two additional oxidation/reduction cycles were completed to ensure that the CO_{ads} was completely removed during the first cycle.

Results and Discussion

Oxidation of HOPG

Ozone oxidation of HOPG. It has been shown in previous work that nano-scale pits can be formed on HOPG by an ozone oxidation process (10). HOPG pitting by O_3 was tested in this work. Consistent with the literature, oxidation of HOPG with O_3 was found to result in nanometre-sized pits that are randomly distributed over the basal plane of the HOPG surface (10). The pit size and density can be controlled by varying the O_3 concentration, reaction time and temperature. An STM image and the corresponding pit size histogram for a HOPG surfaces oxidized for 15 min. at 300 °C and 0.15 ppm O_3 are shown in Figure 1. Under these conditions, the average pit diameter and is 3.8 nm and there are 2400 pits per μm. All ozone oxidized samples shown in the following are oxidized at 15 min. at 300 °C and 0.15 ppm O_3.

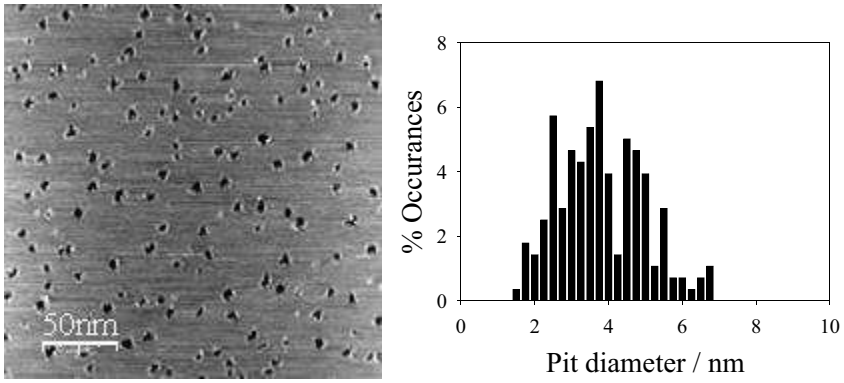

Figure 1. STM images of HOPG surfaces oxidized in 0.15 ppm O_3 at 300 °C for 15 min. The corresponding pit diameter histograms is also shown.

Electrochemical oxidation of HOPG. Electrochemical oxidation of HOPG produced drastically different results than ozone oxidized HOPG. Electrochemical oxidation of HOPG is known to exfoliate the HOPG surface (14,15,16). Exfoliation follows a three step process: Firstly, intercalation of water and electrolyte strain the top-most layer of the atomically flat surface of HOPG. The C–C bonds, which are still intact, become further strained as protrusions begin to appear. Finally, some of the C–C bonds on the top area of the protrusions begin to fracture forming graphite oxide and pits on the HOPG surface. SEM analysis, Figure 2, indicates pits formed on the HOPG surface after 90 s of electrochemical oxidation at 1.55 V vs. MSE in 0.1 M H_2SO_4 are on average 80 nm in diameter.

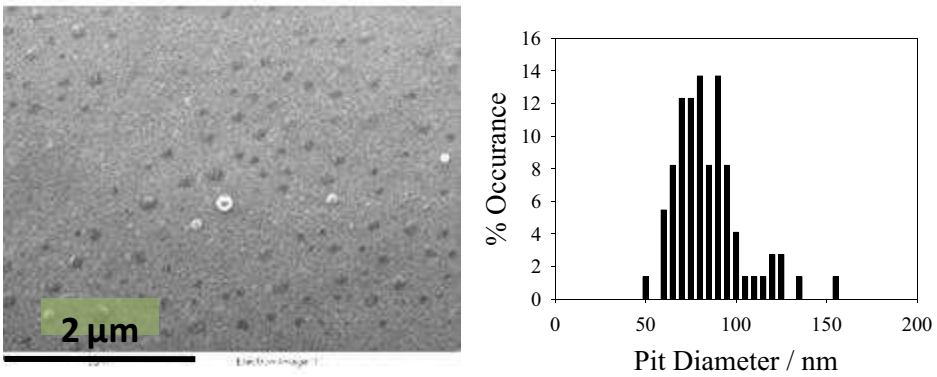

Figure 2. SEM image of HOPG electrochemically oxidized at 1.55 V vs. MSE in 0.1 M H_2SO_4 for 90 s.

Effect of HOPG Oxidation on Nucleation

Analysis of current-time transients for the electrochemical deposition of Pt onto freshly cleaved HOPG substrates indicates that Pt deposition occurs via a 3-D nucleation process. For the majority of nucleation processes, the empirical law

$$\frac{dN}{dt} = AN_0e^{(-At)} \qquad [1]$$

describes the rate of nuclei formation (17). N is the number of nucleation sites, N_0 is the number of sites at the beginning of the deposition process ($t = 0$), and A is the nucleation rate constant. If the nucleation rate is very large ($A >> 1$), integrating the rate law gives $N = N_0$, i.e., the number of nuclei is constant. In this case, nucleation is termed instantaneous since all the nuclei are formed instantaneously at the beginning of the experiment. If the nucleation rate is very slow ($A << 1$), integrating the rate law gives $N = AN_0t$. When the number of nuclei is a function of deposition time, nucleation is termed progressive. Assuming that all the nuclei grow at the same rate, instantaneous nucleation results in mono-size-dispersed particles and is the preferred case in this work.

Using the theory developed by Scharifker and Hills, the current transients can be plotted in reduced variables, $(I/I_M)^2$ vs. t/t_M, to easily determine if nucleation is instantaneous or progressive (18). Reduced variable plots for three separate experiments of electrodeposition onto freshly cleaved HOPG in 0.1 M H_2SO_4 + 1 mM $PtCl_4$ at – 0.475 V vs. MSE, run under the same experimental conditions, are plotted in Figure 3a. It is seen that the three experiments give three different results. Such a large variation in the nucleation process indicates a large variation in the number of nucleation sites on different HOPG substrates.

Plotted in Figure 3b are the reduced variable plots for three separate experiments of constant potential reduction onto ozone oxidized HOPG in 0.1 M H_2SO_4 + 1 mM $PtCl_4$ at – 0.475 V vs. MSE. Comparison of Figures 3a and 3b clearly shows how ozone oxidization of HOPG results in increased reproducibility of the nucleation process.

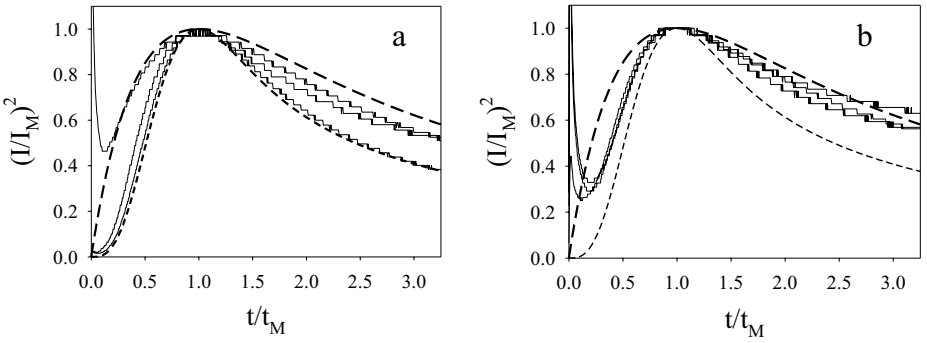

Figure 3. Reduced variable plots (see text) of potentiostatic Pt deposition onto (a) freshly cleaved and (b) ozone oxidized HOPG in 0.1 M H_2SO_4 + 1 mM $PtCl_4$ at – 0.475 vs. MSE. _____ experimental data, _ _ _ theoretical instantaneous nucleation, and - - - - - theoretical progressive nucleation.

Nano-catalyst Morphology

Nano-Catalyst Formed by Constant Potential Deposition. Figure 4 shows TEM images of Pt potentiostatically deposited for 5 s onto freshly cleaved HOPG. The platinum deposits in Figure 4a are on average 80 nm in diameter. A higher resolution image from the same sample is shown in Figure 4b. It indicates that the Pt deposits are in fact agglomerates of nano-catalysts which are on average 3.5 nm in diameter. It is seen, Figure 4a, that the Pt deposits form in lines. As previous work shows that electrochemically deposited platinum forms preferentially on step edges, the lines of agglomerates observed here are assumed to coincide with step edges of the HOPG (13,19,20). Defects in the basal plane can also act as nucleation sites, but on a typical HOPG surface they are far less numerous than step edges.

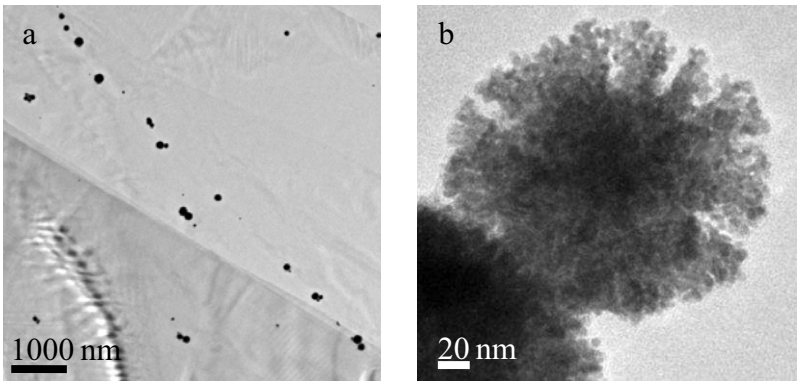

Figure 4. a) TEM images of Pt deposits on freshly cleaved HOPG. The Pt was deposited at – 0.475 V vs. MSE for 5 s in 0.1 M H_2SO_4 + 1 mM $PtCl_4$. b) shows the high resolution TEM image of the same sample.

Oxidizing the HOPG surface, either with ozone gas or electrochemically, resulted in electrodeposition of Pt onto the basal planes. Although neither oxidation method prevented the Pt nano-catalysts from agglomerating, it was found that the agglomerate size could be controlled by controlling the deposition time. For example, on ozone oxidized HOPG the average agglomerate diameter decreased from 100 to 55 to 37 nm for

samples formed at constant potential deposition for 7.5, 5 and 2.5 s respectively. Similar to the case of Pt electrodeposition onto freshly cleaved HOPG, the agglomerates were found to consist of individual particles, suggesting that the particles (and possibly small agglomerates) are mobile on the surface during the deposition process.

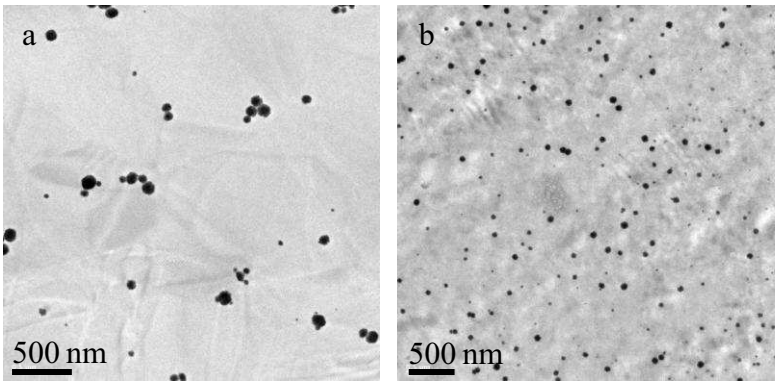

Figure 5. TEM images of Pt deposited at constant potential onto a) ozone oxidized (in 0.15 ppm O_3 for 15 min at 300 °C) HOPG, and b) electrochemically oxidized (at 1.55 V vs. MSE for 90 s in 0.1 M H_2SO_4) HOPG. For both samples, the Pt was deposited at – 0.475 V vs. MSE for 5 s in 0.1 M H_2SO_4 + 1 mM $PtCl_4$.

Nano-Catalysts Formed by Thermal Decomposition. Thermal decomposition proved to be a much more successful deposition technique as the deposition process did not result in the formation of Pt agglomerates; instead, well dispersed nano-catalyst were formed. Figure 6 shows TEM images of Pt nano-catalysts prepared by thermal decomposition onto HOPG. The HOPG substrate was pre-oxidized by either ozone gas (Figure 6a) or electrochemically (Figure 6b). Both substrate oxidation methods produced well dispersed Pt nano-catalysts. Pt nano-catalysts formed using 175 μL 6.5×10^{-5} M HCl + 2.6×10^{-5} M H_2PtCl_4 were 4.2 ± 1 and 2.3 ± 0.5 nm on the ozone and electrochemically oxidized substrates respectively.

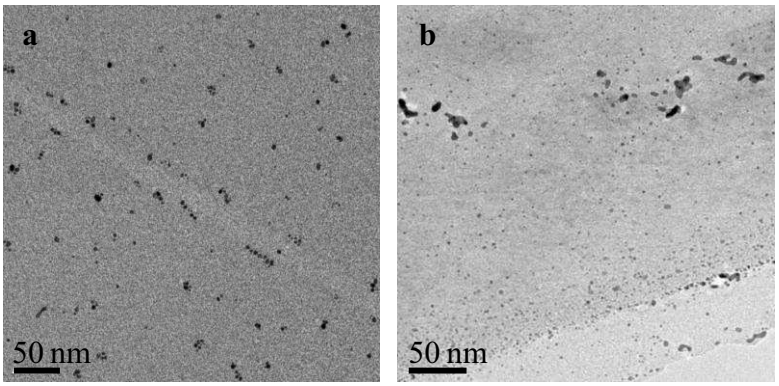

Figure 6. TEM images of Pt nano-catalyst formed by thermal decomposition onto a) ozone oxidized (in 0.15 ppm O_3 for 15 min. at 300 °C) HOPG, and b) electrochemically oxidized (at 1.55 V vs. MSE for 90 s in 0.1 M H_2SO_4) HOPG. For both samples, 175 μL 6.5×10^{-5} M HCl + 2.6×10^{-5} M H_2PtCl_4 was pipetted onto the substrates, allowed to air dry, and reduced under hydrogen at 250 °C.

Thermal decomposition is known to make nano-catalysts on HOPG, however, the nano-catalysts reported in literature agglomerated when cycling the potential between the regions of hydrogen and oxygen evolution (11). To test the stability of the thermally decomposed nano-catalysts prepared in this work, TEM analysis was completed on samples prepared in the same manner as the samples in Figure 6 that also underwent CO_{ads} stripping voltammetry. The average Pt nano-catalyst size formed by thermal decomposition on electrochemically oxidized HOPG after CO_{ads} stripping voltammetry is 26.5 ± 6.5 nm, which is more than an order of magnitude larger than the as-prepared sample which did not undergo CO_{ads} stripping voltammetry. It is important to emphasize that the TEM analysis procedure is a destructive technique. Thus, it is impossible to image the same sample before and after stripping voltammetry. Consequently, we cannot determine if stripping voltammetry causes the platinum nano-catalyst to agglomerate, or if the deposition technique is irreproducible. Regardless, HOPG that has been electrochemically oxidized, does not facilitate the production of a model catalyst system. Conversely, it was found that the Pt nano-catalysts prepared by thermal decomposition, in the same manner as the sample in Figure 6a, i.e., onto ozone oxidized HOPG and that has undergone CO_{ads} stripping voltammetry, are the same size (4.4 ± 1.4 nm) as the as-prepared sample. Thus, thermal decomposition of Pt onto ozone oxidized HOPG is the superior sample preparation technique.

CO_{ads} Oxidation Characteristics

The activity of the various Pt/HOPG samples towards oxidizing adsorbed carbon monoxide was studied. Figure 7a shows the stripping voltammograms for the oxidation of carbon monoxide adsorbed onto the platinum nano-catalyst prepared by constant potential deposition onto ozone and electrochemically oxidized HOPG. The stripping voltammogram for the oxidation of carbon monoxide adsorbed onto polycrystalline bulk platinum is included for comparison. The CO_{ads} oxidation characteristics are remarkably similar for the two nanocatalyst samples prepared by electrodeposition despite the different substrate oxidation procedures. In both cases, the oxidation onset potential is shifted to higher potentials compared to polycrystalline bulk platinum. This possibly indicates that it is more difficult to form adsorbed hydroxyl groups on the nano-catalyst compared to polycrystalline bulk platinum. This result contrasts with work in literature that has shown that Pt agglomerates have similar adsorbed carbon monoxide oxidation characteristics to polycrystalline bulk platinum (21).

Figure 7b shows the stripping voltammograms for the oxidation of carbon monoxide adsorbed onto the platinum nano-catalyst prepared by thermal decomposition onto ozone and electrochemically oxidized HOPG. As with Figure 7a, the stripping voltammogram for the oxidation of carbon monoxide adsorbed onto polycrystalline bulk platinum is included for comparison. The stripping voltammograms for the Pt nano-catalyst formed by thermal decomposition are very similar to one another regardless of the substrate oxidation technique, and notably different than the stripping voltammograms for platinum nano-catalysts formed at constant potential. This indicates that the substrate pre-treatment does not play a significant role towards the electro-catalytic behaviour of the platinum nano-catalyst; rather, the Pt fabrication technique is important. The onset of the CO_{ads} oxidation reaction on the Pt nano-catalysts formed by thermal decomposition occurs at potentials more negative than polycrystalline bulk platinum possibly indicating that hydroxyl formation occurs more readily on the Pt nano-catalysts compared to

polycrystalline bulk platinum. The overall oxidation kinetics are faster for the Pt nano-catalysts formed by thermal decomposition compared to polycrystalline bulk platinum. Also, there are two distinct CO_{ads} stripping peaks for the Pt nano-catalysts formed by thermal decomposition, while the nano-catalysts formed at constant potential only had one oxidation peak.

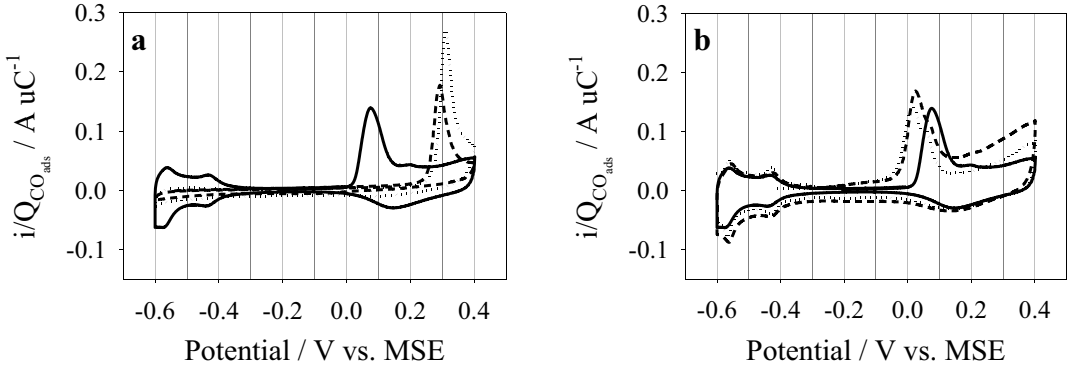

Figure 7. CO_{ads} stripping CV recorded at 10 mV s^{-1} with the current normalized by the corresponding stripping charge. a) Shows CO_{ads} stripping voltammograms for Pt deposited at– 0.475 V vs. MSE in 0.1 M H_2SO_4 + 1 mM $PtCl_4$ for 5 s onto ..... ozone oxidized HOPG, and _ _ _ _ _ electrochemically oxidized HOPG. b) Shows CO_{ads} stripping voltammograms for Pt decomposed thermally (250 µL of 2.6×10^{-4} M H_2PtCl_4 + 6.4×10^{-4} M HCl) onto ..... ozone oxidized HOPG, and (250 µL of 2.6×10^{-5} M H_2PtCl_4 + 6.5×10^{-5} M HCl) _ _ _ _ _ electrochemically oxidized HOPG. Included for comparison on both figures is the CO_{ads} stripping voltammogram for polycrystalline bulk Pt _____. Ozone oxidation of the substrate was carried out in 0.15 ppm O_3 at 300 °C for 15 min, while electrochemical oxidation occurred in 0.1 M H_2SO_4 at 1.55 V vs. MSE for 30 s.

Electrochemical Stability

The electrochemical stability of the Pt nano-catalysts was tested by running five successive CO_{ads} oxidation stripping voltammograms on each of the four different samples. The percent loss of stripping charge was calculated as

$$\% \text{ loss } CO_{ads} \text{ oxidation charge} = \frac{Q_1st - Q_nth}{Q_1st} \times 100 \quad [2]$$

Table 1 lists the percentage loss of CO_{ads} oxidation charge with each successive stripping voltammogram. The sample prepared by constant potential deposition onto freshly cleaved HOPG has the lowest electrochemical stability. Over 90 % of the stripping charge from the first CO_{ads} stripping voltammogram is lost by the fifth CO_{ads} stripping voltammogram. A loss of CO_{ads} oxidation charge indicates a loss of Pt surface area, thus over the course of five CO_{ads} stripping voltammograms, over 90 % of the Pt surface areas is lost either due to agglomeration, dissolution, or a combination of both. The samples prepared at constant potential onto oxidized HOPG are not significantly more electrochemically stable, they lost approximately 70 % of the stripping charge by the fifth CO_{ads} stripping voltammogram.

Comparing the samples prepared on electrochemically oxidized HOPG at constant potential and by thermal decomposition, it is seen that the latter is twice as stable as the nano-catalyst prepared at constant potential. Furthermore, the sample prepared by thermal decomposition of Pt onto ozone oxidized HOPG has negligible loss of stripping charge over the five experiments indicating a negligible loss in Pt surface area. From the electrochemical stability data, it is clear that the most promising method of preparing platinum nano-catalyst on HOPG is to thermally decompose Pt onto ozone oxidized HOPG.

TABLE I. Comparison of the loss of CO_{ads} stripping charge

HOPG Treatment	Pt Nano-catalyst Preparation	% loss of CO_{ads} Oxidation Charge			
		2nd	3rd	4th	5th
Freshly Cleaved	Constant Potential Deposition*	47	81	90	96
Electrochemically Oxidized†	Constant Potential Deposition‡	19	39	64	64
Ozone Oxidized§	Constant Potential Deposition*	46	64	66	70
Electrochemically Oxidized†	Thermal Decomposition**	1	10	19	36

* Pt was deposited at – 0.475 V vs. MSE in 0.1 M H_2SO_4 + 1 mM $PtCl_4$ solution for 7.5 s.
† 30 s electrochemical oxidation at 1.55 V vs. MSE in 0.1 M H_2SO_4.
‡ Pt was deposited at – 0.475 V vs. MSE in 0.1 M H_2SO_4 + 1 mM $PtCl_4$ solution for 5 s.
§ HOPG was oxidized at 300 °C for 15 min in 0.15 ppm O_3.
** 250 µL of 2.6×10^{-5} H_2PtCl_4 + 6.5×10^{-5} HCl.

Conclusions

Within this work, we have studied electrodeposition and thermal decomposition as two different methods to form Pt nano-catalysts. The nano-catalysts were prepared on HOPG oxidized either by ozone gas or electrochemically. As a point of reference, the morphology, the activity towards electrochemical oxidation of CO_{ads}, and the electrochemical stability of the Pt nano-catalysts were compared to those of Pt nano-catalysts formed by electrodeposition onto freshly cleaved HOPG.

It was found that oxidizing the HOPG substrate with ozone gas greatly improved the reproducibility of the Pt nucleation process. Electrodeposition, under the conditions used in this work, resulted in the agglomeration of Pt nano-catalysts. Neither ozone nor electrochemical oxidation pre-treatment of the HOPG substrate was able to prevent agglomeration of the Pt nano-catalyst during their electrodeposition. However, the agglomerate size could be controlled by varying the deposition time. Thermal decomposition onto ozone and electrochemically oxidized HOPG produced well dispersed nano-catalysts that did not agglomerate during the deposition process. However, TEM analysis revealed that thermal decomposition onto electrochemically oxidized HOPG is either an irreproducible deposition technique or the electrochemically oxidized substrate is not capable of stabilizing the nano-catalysts from agglomeration during CO_{ads} stripping voltammetry. Thermal decomposition onto ozone oxidized HOPG, however, produced Pt nano-catalysts that are stable towards agglomeration during CO_{ads} stripping voltammetry. Thermal decomposition onto ozone oxidized HOPG is also very reproducible.

Analysis of the oxidation characteristics of CO_{ads} by stripping voltammetry revealed that the electrochemical behaviour of the Pt nano-catalyst is more greatly influenced by the deposition technique than by the substrate oxidation characteristics. The onset

potential for CO_{ads} was observed to be more positive for nano-catalysts prepared by electrodeposition at constant potential than polycrystalline bulk platinum. This possibly indicates that it is more difficult to form adsorbed OH on the nano-catalysts than on polycrystalline bulk platinum. Overall the CO_{ads} oxidation kinetics were slower on the nano-catalyst prepared by electrodeposition compared to polycrystalline bulk Pt. The CO_{ads} oxidation onset for Pt-nano-catalyst prepared by thermal decomposition, however, were shifted to lower potentials compared to polycrystalline bulk platinum possibly indicating that adsorbed OH groups form more easily on the nano-catalysts formed by thermal decomposition. The CO_{ads} oxidation kinetics on these Pt nano-catalysts is faster than the CO_{ads} oxidation kinetics on polycrystalline bulk platinum.

Electrochemical stability analysis indicated that the Pt nano-catalysts prepared by thermal decomposition onto ozone oxidized HOPG are the most stable against loss of Pt surface area during successive CO_{ads} stripping voltammetry. Hence, thermal decomposition onto ozone oxidized HOPG is the superior preparation techniques to make this type of model nano-catalysts.

Acknowledgments

The authors thank David Kingston for XPS and SEM analysis of selected samples. We would also like to acknowledge the Ontario Graduate Student Scholarship program and the NRC-Helmholtz and the Trilateral NRC-ITRI-NSC funds for financial support.

References

1. R. I. Masel, *Chemical Kinetics and Catalysis,* Wiley-Interscience, Toronto (2001).
2 . K. Bergamaski, A. L. N. Pinheiro, E. Teixeira-Neto and F.C. Nart, *J. Phys. Chem. B.* , **110**, 19271 (2006).
3. H. A. Gasteiger, S. S. Kocha, B. Sompalli and F.T. Wagner, *Applied Catalysis B.*, **56,** 9 (2005).
4. F. Maillard, M. Martin, F. Gloaguen and J.M. Leger, *Electrochim. Acta*, **47**, 3431 (2002).
5. K. Kinoshita, *J. Electrochem. Soc.*, **137**, 485 (1990).
6. M. Watanabe, H. Sei, P. Stonehart, *J. Electroanal. Chem.*, **261**, 375 (1989).
7. J. V. Zoval, J. Lee, S. Gorer and R.M. Penner, *J. Phys. Chem. B*, **102**, 1166 (1998).
8. P. Shen, N. Chi, K.-Y. Chan and D. L. Phillips, *Applied Surface Science*, **172**, 159 (2001).
9. S. Liu, Z. Tang, E. Wang and S. Dong, *Electrochem. Commun.* **2**, 800 (2000).
10. A. Tracz, G. Wegner and J. P. Rabe, *Langmuir*, **19**, 6807 (2003).
11. E. R. Savinova, N. P. Levedeva, P. A. Simonoc and G. N. Kryukova, *Russ. J. Electrochem.*, **36**, 952 (2000).
12. K. Kinoshita, *Carbon: Electrochemical and Physicochemical Properties,* Wiley, New York (1988).
13. Z. Siroma, K. Ishii, K. Yasuda, Y. Mayazaki, M. Inaba and A. Tasaka, *Electrochem. Commun.*, **7**, 1153 (2005)

14. B. Zhang, E. Wang, *Electrochim. Acta*, **40**, 2627 (1995).
15. C. A. Goss, J. C. Brumfield, E. A. Irene, R. W. Murray, *Anal. Chem.*, **65**, 1378 (1993).
16. K. W. Hathcock, J. C. Brumfield, C. A. Goss, E. A. Irene, R. W. Murray, *Anal. Chem.*, **67**, 2201 (1995).
17. M. Fleischmann and H.R. Thirsk, *Trans. Faraday Soc*. **51**, 71 (1955).
18. B. Scharifker and G. Hills, *Electrochim. Acta*, **28**, 879 (1983).
19. J. V. Zoval, J. Lee, S. Gorer and R. M. Penner, *J. Phys. Chem B*, **102**, 1166 (1998).
20. G. Lu and G. Zangari, *Electrochim. Acta*, **51,** 2531 (2006).
21. F. Maillard, S. Schreier, M. Hanzlik, E.R. Savinova, S. Weinkauf and U. Stimming, *Phys. Chem. Chem. Phys.*, **7**, 385 (2005).